Topology and Operation Modes of Magnetically Integrated Switched Inductor Boost Converters

Zhiwei Li[1,*], Yuxin Wan[2] and Wenxuan Wu[3]

[1] School of Physics & Optoelectronic Engineering, Guangdong University of Technology, Guangzhou, China
[2] International College, Beijing University of Posts and Telecommunications, Beijing, China
[3] Department of Automation Engineering, Zhonghuan Information College Tianjin University of Technology, Tianjin, China
*3221007128@mail2.gdut.edu.cn

Abstract. Recent years have witnessed a growing interest in altering the connection configuration of converters to enhance the electrical efficiency of boost converters within DC-DC converter systems. This paper explores three connection methods for the magnetic integrated switched inductor boost converter: staggered parallel connection, single switched inductor cascade, and double switched inductor cascade. The study introduces these topologies and operation modes, emphasizing their enhancements in terms of voltage gain and inductor current ripple compared to traditional boost converters. Additionally, it summarizes existing research on these connection modes, providing insights for further advancements in this field. The necessity for developing and utilizing new energy sources amid the energy crisis is underscored, with DC-DC converters being pivotal in new energy power generation systems. Boost converters, particularly, have garnered attention due to their efficiency and compactness, prompting extensive research globally. Various strategies, including magnetic integration technology, have been explored to improve these converters, aiming to increase voltage gain and reduce inductor current ripple. Comparative analyses of different connection modes reveal significant advancements, especially in voltage gain, highlighting the potential of these approaches in enhancing the performance of new energy systems. Through tightly coupling discrete inductors using magnetic integration, the proposed converter demonstrates improved electrical performance, making it suitable for various high-gain DC-DC converter applications in new energy systems.

Keywords: DC-DC Converter, Boost Converter, Interleaved Parallel Connection, Switched Inductor Cascade Connection.

1 Introduction

Since the Industrial Revolution, the rapid development of society and national economy has been accompanied by the over-collection and consumption of traditional energy. Therefore, it is necessary to fully develop and utilize new energy sources to cope with the energy crisis [1]. At present, the research of all kinds of new energy

Y. Yue (ed.), *Proceedings of the 2024 International Conference on Mechanics, Electronics Engineering and Automation (ICMEEA 2024)*, Advances in Engineering Research 240,
https://doi.org/10.2991/978-94-6463-518-8_37

power generation system has become a hot topic all over the world [2]. DC-DC converter (DC-DC converter) is an important energy conversion device in new energy power generation system. Among the DC-DC converters, the boost converter has been intensively studied because of its high transmission efficiency and easy volume reduction, and has been widely used in the field of low-voltage power generation systems [3]. Domestic and foreign scholars have done a lot of research in the field of Boost converter. Literature [4,5] have given us a preliminary understanding of high gain converters by means of classification discussion and deduction of topology. Some scholars have spent by the combination of units, multi-input to achieve high gain, but also need to bear the high cost of power [6]. Based on the traditional Boost converter, the energy storage capacitor module is introduced to replace the original energy storage inductor unit, and its phase-shifting control is also a good improvement method, however, the current ripple of the inductor is still large, and the voltage gain is not significant [7,8]. The high gain of the converter is realized by coupling, and various methods are adopted to overcome the disadvantage of high voltage stress of the switch caused by the coupling inductor, this is highly in line with the expected improvements, but often such circuit designs can make the circuit structure too cumbersome to control [9,10].

In this paper, based on the traditional Boost converter, the magnetic integration technology [11] is used to introduce the switch inductor module to reduce the ripple of inductor current, in order to improve the transient response of the converter and the volume of the converter.

2 Comparison of Various Connection Methods for Converter

Different converter topologies of high gain DC-DC converters are proposed in the past twenty years [12]. The high gain boost converter has various connection methods which include staggered parallel connection method and cascade connection method. The following section analyses the topology, voltage gain and inductor current ripple of these three types of connections.

2.1 Interleaved Connection Mode

This connection can increase the voltage gain of Boost converter effectively and reduce the inductive current ripple of the converter [13]. In addition, introducing switched inductor module into the staggered parallel Boost converter is conducive to further improving the conversion efficiency of the converter [13].

The Analysis of Operational Mode. It can be seen that there are four operating modes of the circuit when the two magnetically integrated switched inductor boost converters are connected by staggered parallel connection. The component states for

each operating mode are shown in Table 1, Table 2 as well as Table 3, while the topologies are shown in Fig. 1, Fig. 2 and Fig. 3.

The individual voltage relation equations for Mode 1 are

$$\begin{cases} L\frac{di_{L_1}}{dt}+M_1\frac{di_{L_2}}{dt}+M_2\frac{di_{L_3}}{dt}+M_2\frac{di_{L_4}}{dt}=V_{in} \\ M_1\frac{di_{L_1}}{dt}+L\frac{di_{L_2}}{dt}+M_2\frac{di_{L_3}}{dt}+M_2\frac{di_{L_4}}{dt}=V_{in} \\ M_2\frac{di_{L_1}}{dt}+M_2\frac{di_{L_2}}{dt}+L\frac{di_{L_3}}{dt}+M_1\frac{di_{L_4}}{dt}=\frac{V_{in}+V_C-V_o}{2} \\ M_2\frac{di_{L_1}}{dt}+M_2\frac{di_{L_2}}{dt}+M_1\frac{di_{L_3}}{dt}+L\frac{di_{L_4}}{dt}=\frac{V_{in}+V_C-V_o}{2} \end{cases} \tag{1}$$

The individual voltage relations for Modes 2 and 4 are:

$$\begin{cases} L\frac{di_{L_1}}{dt}+M_1\frac{di_{L_2}}{dt}+M_2\frac{di_{L_3}}{dt}+M_2\frac{di_{L_4}}{dt}=\frac{V_{in}+V_C-V_o}{2} \\ M_1\frac{di_{L_1}}{dt}+L\frac{di_{L_2}}{dt}+M_2\frac{di_{L_3}}{dt}+M_2\frac{di_{L_4}}{dt}=\frac{V_{in}+V_C-V_o}{2} \\ M_2\frac{di_{L_1}}{dt}+M_2\frac{di_{L_2}}{dt}+L\frac{di_{L_3}}{dt}+M_1\frac{di_{L_4}}{dt}=\frac{V_{in}+V_C-V_o}{2} \\ M_2\frac{di_{L_1}}{dt}+M_2\frac{di_{L_2}}{dt}+M_1\frac{di_{L_3}}{dt}+L\frac{di_{L_4}}{dt}=\frac{V_{in}+V_C-V_o}{2} \end{cases} \tag{2}$$

At last, it can be known that the individual voltage relations for Modes 3 as below:

$$\begin{cases} L\frac{di_{L_1}}{dt}+M_1\frac{di_{L_2}}{dt}+M_2\frac{di_{L_3}}{dt}+M_2\frac{di_{L_4}}{dt}=\frac{V_{in}+V_C-V_o}{2} \\ M_1\frac{di_{L_1}}{dt}+L\frac{di_{L_2}}{dt}+M_2\frac{di_{L_3}}{dt}+M_2\frac{di_{L_4}}{dt}=\frac{V_{in}+V_C-V_o}{2} \\ M_2\frac{di_{L_1}}{dt}+M_2\frac{di_{L_2}}{dt}+L\frac{di_{L_3}}{dt}+M_1\frac{di_{L_4}}{dt}=V_{in} \\ M_2\frac{di_{L_1}}{dt}+M_2\frac{di_{L_2}}{dt}+M_1\frac{di_{L_3}}{dt}+L\frac{di_{L_4}}{dt}=V_{in} \end{cases} \tag{3}$$

Table 1. Operating states of field effect tubes in staggered parallel connection mode.

Operating mode	S_1	S_2
Mode 1	On	Off
Mode 2/4	Off	Off
Mode 3	Off	On

Table 2. Operating states of diodes in staggered parallel connection mode.

operating mode	D_1	D_2	D_3	D_4	D_5	D_6	D_7	D_8	D_9	D_{10}
Mode 1	√	×	√	×	√	×	√	×	×	√
Mode 2/4	×	√	×	×	√	×	×	×	√	√
Mode 3	×	√	×	√	×	√	×	√	√	×

√：on ×：off

Table 3. Changes in inductor current for staggered parallel connection.

operating mode	i_{L_1}	i_{L_2}	i_{L_3}	i_{L_4}
Mode 1	+	+	-	-
Mode 2/4	-	-	-	-
Mode 3	-	-	+	+

+: increase -: decrease

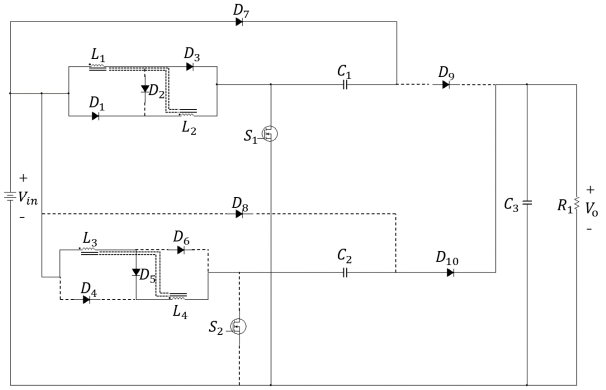

Fig. 1. The topology of Mode 1 [3]

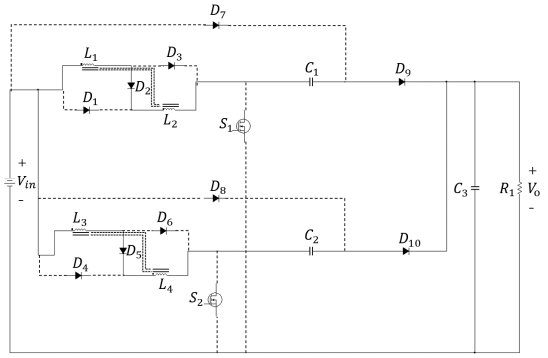

Fig. 2. The topology of Mode 2 and Mode 4 [3].

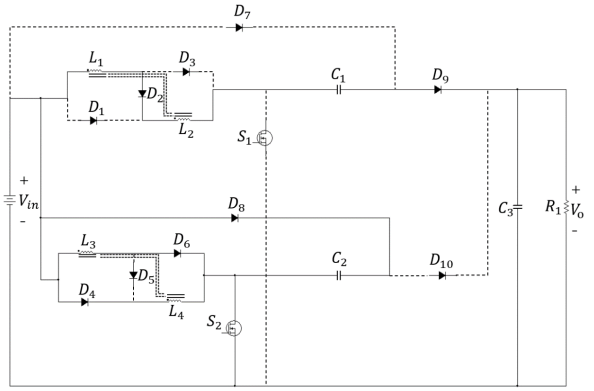

Fig. 3. The topology of Mode 3 [3]

The Analysis of Voltage Gain. Firstly, it is assumed that D is the duty cycle of the field effect tubes S_1 and S_2 in one operating cycle, and T is one operating cycle. So, in Mode 1, the operating time is DT. And it is possible to know that the rate of change of the current i_{L_1} is

$$\frac{di_{L_1}}{dt} = \frac{(L+M_1-2M_2)V_{in}-V_oM_2}{(L+M_1)^2-4{M_2}^2} \tag{4}$$

And in Mode 2 and Mode 4, the total of operating time is $（1-2D）T$. Moreover, it can be seen that the rate of change of the current i_{L_1} is

$$\frac{di_{L_1}}{dt} = \frac{2V_{in}-V_o}{2（L+M_1+2M_2）} \tag{5}$$

Lastly, in Mode 3, the total of operating time is DT and it can be seen that the rate of change of the current i_{L_1} is:

$$\frac{di_{L_1}}{dt} = \frac{2(L+M_1-2M_2)V_{in}+0.5(L+M_1)V_o}{(L+M_1)^2-4{M_2}^2} \tag{6}$$

During an operating cycle, the voltage gain is $\frac{V_o}{V_{in}} = \frac{2}{1-D}$.

The Analysis of Inductive Current Ripple. Firstly, in one operating cycle, the equivalent steady-state inductors of the branch are set to be L_{eq1}~L_{eq4} and the operating frequency of the field effect tube to be f_s. When connection of the circuit is uncoupled, it is assumed that the independent inductance is L_{dis}.

When the resistance value of the load connected to the DC converter is suddenly increased, the response speed of the converter can be improved by increasing the duty cycle of each field effect tube. When the duty cycle of the field effect tube is

increased by ΔD, the amount of change of current in the branch of circuit for each time period can be obtained as follows:

$$t_0 \sim t_1: \ \Delta i_{L_{11}} = \left(\frac{V_1}{L_{eq1}} - \frac{V_{in}-0.5V_o}{L_{eq2}}\right)\frac{\Delta D}{f_s} \tag{7}$$

$$t_1 \sim t_2: \ \Delta i_{L_{12}} = \left(\frac{V_{in}-0.5V_o}{L_{eq2}} - \frac{V_{in}-0.5V_o}{L_{eq2}}\right)\frac{0.5-D-\Delta D}{f_s} = 0 \tag{8}$$

$$t_2 \sim t_3: \ \Delta i_{L_{13}} = \left(\frac{V_{in}-0.5V_o}{L_{eq3}} - \frac{V_{in}-0.5V_o}{L_{eq3}}\right)\frac{\Delta D}{f_s} = 0 \tag{9}$$

$$t_3 \sim t_4: \ \Delta i_{L_{14}} = \left(\frac{V_{in}-0.5V_o}{L_{eq3}} - \frac{V_{in}-0.5V_o}{L_{eq4}}\right)\frac{\Delta D}{f_s} \tag{10}$$

$$t_4 \sim t_5: \ \Delta i_{L_{15}} = \left(\frac{V_{in}-0.5V_o}{L_{eq4}} - \frac{V_{in}-0.5V_o}{L_{eq4}}\right)\frac{0.5-D-\Delta D}{f_s} = 0 \tag{11}$$

Then the sum of the increases in current i_{L_1} is:

$$\Delta i_{L_1} = \Delta i_{L_{11}} + \Delta i_{L_{12}} + \Delta i_{L_{13}} + \Delta i_{L_{14}} + \Delta i_{L_{15}} = \frac{0.5V_o}{L_{eq2}}\frac{\Delta D}{f_s} \tag{12}$$

When the inductive winding method of the converter is uncoupled and the duty cycle of field effect tube increases ΔD, it can be obtained that:

$$\Delta i'_{L_{11}} = \frac{V_{in}\Delta D}{L_{dis}f_s} \tag{13}$$

$$\Delta i'_{L_{12}} = \frac{V_{in}-0.5V_o\Delta D}{L_{dis}f_s} \tag{14}$$

After associating equations (13) and (14), it can be obtained that:

$$\Delta i'_{L_1} = \frac{0.5V_o\Delta D}{L_{dis}f_s} \tag{15}$$

By comparing equations (12) and (15), it can be seen that the difference between the transient currents of the branch under coupled and uncoupled connections is mainly due to the fact that $L_{eq2} \neq L_{dis}$.

When the inductive winding method of the converter is coupled, the steady current ripple of branch L_1 is:

$$\Delta I'_{L_1} = \frac{V_{in}D}{L_{eq1}f_s} \tag{16}$$

When it is uncoupled, the steady current ripple of branch L_1 is:

$$\Delta I'_{L_1} = \frac{V_1\Delta D}{L_{dis}f_s} \tag{17}$$

From equations (15) and (17), it can be seen that when the connection is uncoupled, steady inductance and transient inductance of the branch of the converter

are both L_{dis}. Therefore, reducing the branch steady current ripple and increasing the response speed of the system cannot be satisfied at the same time.

However, from equations (12) and (16), it is possible to reduce inductance current ripple of branch and increase response speed of the system at the same time.

2.2 Connection of a Single Switched Inductor Cascade

A cascaded boost converter typically has a higher voltage gain than a conventional boost converter. This design makes the total gain of the entire cascade structure equal to the product of the individual gains of the components.

The Analysis of Operational Mode. It is assumed that the currents in both inductors are continuous. During a complete cycle T, the converter contains two main operating modes [14]. The topology of operating modes is depicted in Fig. 4 and Fig. 5 respectively as well as the operating states of components are shown in Table 4, Table 5 and Table 6.

The voltage equations for each loop of operating Mode $1[t_0 \sim t_1]$ are presented in Equation (18).

$$\begin{cases} L_1 \frac{di_{L_1}}{dt} + M \frac{di_{L_2}}{dt} = V_m \\ M \frac{di_{L_1}}{dt} + L_2 \frac{di_{L_2}}{dt} = V_{in} \\ L_3 \frac{di_{L_3}}{dt} = u_{C_1} \\ u_{C_2} = V_o \end{cases} \tag{18}$$

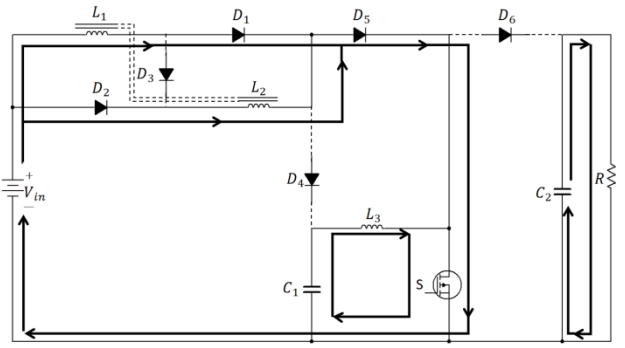

Fig. 4. Operating Modes $1(t_0 \sim t_1)$ [14].

For the same reason, the voltage equations for each loop of Mode $2(t_1 \sim t_2)$ are given in Equation (19).

$$\begin{cases} L_1\frac{di_{L_1}}{dt}+M\frac{di_{L_2}}{dt}+L_2\frac{di_{L_2}}{dt}+M\frac{di_{L_1}}{dt}=u_{C_1}-V_n \\ L_1\frac{di_{L_1}}{dt}+M\frac{di_2}{dt}+L_2\frac{di_{L_2}}{dt}+M\frac{di_{L_1}}{dt}+L_3\frac{di_{L_3}}{dt}=V_o-V_n \\ u_{C_2}=V_o \end{cases} \tag{19}$$

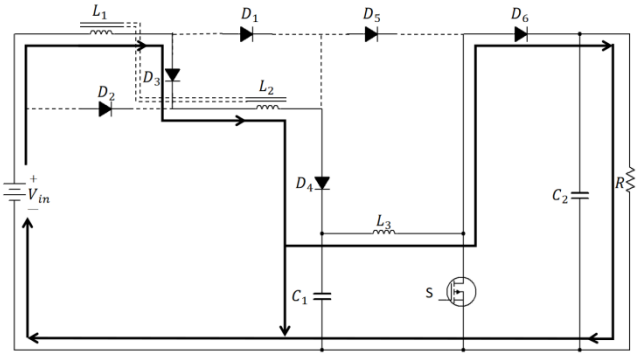

Fig. 5. Operating Modes 2 (t_1~t_2) [14].

Table 4. Operating states of field effect tubes with single switch inductor cascade connection method.

operating mode	S
Mode 1	On
Mode 2	OFF

Table 5. Operating states of diodes in single switch inductor cascade connection mode.

operating mode	D_1	D_2	D_3	D_4	D_5	D_6
Mode 1	√	√	×	×	√	×
Mode 2	×	×	√	√	×	√

√： on ×： off

Table 6. Variation of inductor current for single switch inductor cascade connection method

operating mode	i_{L_1}	i_{L_2}	i_{L_3}
Mode 1	+	+	+
Mode 2	−	−	−

+: increase -: decrease

The Analysis of Voltage Gain. Since this type of converter boost converter replaces inductors L_1 and L_2 in the conventional cascaded boost converter by using a single switched inductor, inductors L_1 and L_2 operate in such a way that, assuming $L_1 = L_2 =$ L, the current gain and loss expressions for L_1, L_2 and L_3 can be derived from Eqs. (18) and (19) as [14]:

$$\begin{cases} \Delta i_{L_1+} = \Delta i_{L_2+} = \frac{V_{in}}{L+M} DT \\ \Delta i_{L_3+} = \frac{u_{C_1}}{L_3} DT \end{cases} \tag{20}$$

$$\begin{cases} \Delta i_{L_1-} = \Delta i_{L_2-} = \frac{u_{C_1} - V_{in}}{2(L+M)} (1-D)T \\ \Delta i_{L_3-} = \frac{V_o - u_{C_1}}{L_3} (1-D)T \end{cases} \tag{21}$$

Equations (20) and (21) can be used to derive the voltage gain:

$$M = \frac{V_o}{V_{in}} = \frac{1+D}{(1-D)^2} \tag{22}$$

From equation (22), the voltage gain of this converter is improved by a factor of (1+D) over the basic cascaded converter.

Analysis of inductive current ripple. According to the previous discussion, the mutual inductance M affects the current ripple Δi_{L_1} of the inductors L_1 and L_2 and the current ripple Δi_{L_1} is related not only to the self-inductance of the inductors L_1 and L_2, but also to the mutual inductance M. The current ripple of Δi_{L_3} inductor L_3 is determined only by its self-inductance L_3. Assuming that the coupling between inductors L_1 and L_2 is given by k:

$$k = \frac{M}{\sqrt{L_1 L_2}} = \frac{M}{L} \tag{23}$$

According to Eq. (22) and Eq. (23), the current ripple of the inductors L_1 ,L_2 and L_3 in the rising phase of the inductor current is obtained as:

$$\begin{cases} \Delta i_{L_4} = \Delta i_{L_2} = \frac{V_{in}}{L(1+k)} DT = \frac{1}{1+k} \Delta i_L^{'} \\ \Delta i_{L_3} = \frac{u_{C_1}}{L_3} DT \end{cases} \tag{24}$$

In equation (24), $\Delta i_L^{'}$ is the ripple of the inductors L1 、 L2 before inductor integration.

$$\varepsilon = \frac{1}{1+k} \tag{25}$$

ε is the inductance ripple reduction factor that satisfies: $0 < \varepsilon < 1$, the ripple size of the inductors L_1 and L_2 will vary with the value of the coupling factor k. The relationship between ε and k is shown in Fig.6.

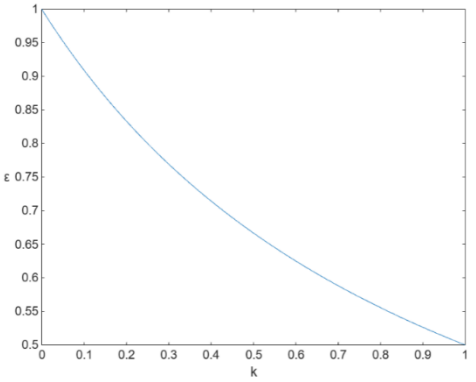

Fig. 6. Plot of k vs ε.

From the analysis in Fig. 6, it can be seen that the ripple factor ε of the inductor current tends to decrease as the coupling factor k approaches 1, and when k reaches 1, the ripple factor decreases to 0.5, which means that when the two inductors L_1 and L_2 are fully coupled, the current ripple is only half of its original value. Therefore, when designing magnetic components in integrated circuits, L_1 and L_2 should be coupled as closely as possible.

2.3 Connection of a Two-Switch Inductive Cascade

The Analysis of Operational Mode. In a switching cycle, there are two operating modes in the converter [15]. There are two different switching modes shown in the following Fig. 7 and Fig. 8. In addition, the operating status of each circuit component is shown in the Table 7, Table 8, and Table 9.

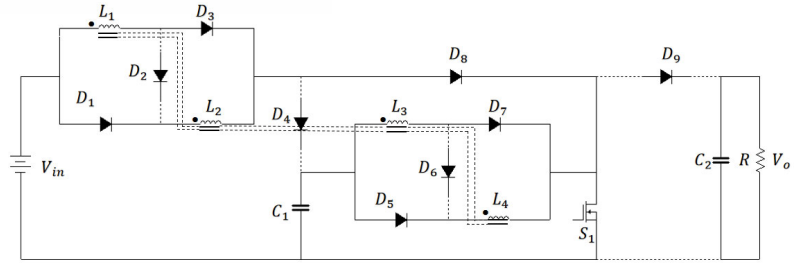

Fig. 7. Operational Modal 1 (t_0~t_1) [15].

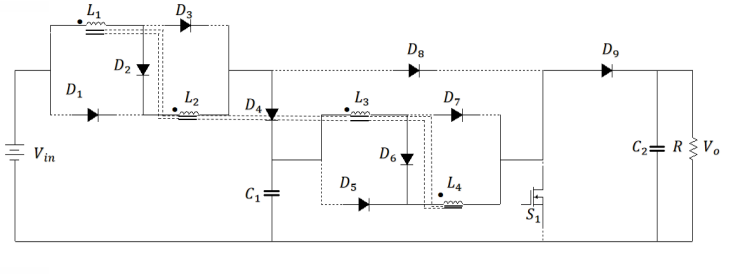

Fig. 8. Operational Modal 2 [t_1~t_2] [15].

The circuit expression of Mode 1 is:

$$\begin{cases} L\frac{di_{L_1}}{dt} + M_1\frac{di_{L_2}}{dt} + M_2\frac{di_{L_3}}{dt} + M_2\frac{di_{L_4}}{dt} = V_{in} \\ M_1\frac{di_{L_1}}{dt} + L\frac{di_{L_2}}{dt} + M_2\frac{di_{L_3}}{dt} + M_2\frac{di_{L_4}}{dt} = V_{in} \\ M_2\frac{di_{L_1}}{dt} + M_2\frac{di_{L_2}}{dt} + L\frac{di_{L_3}}{dt} + M_1\frac{di_{L_4}}{dt} = V_{C1} \\ M_2\frac{di_{L_1}}{dt} + M_2\frac{di_{L_2}}{dt} + M_1\frac{di_{L_3}}{dt} + L\frac{di_{L_4}}{dt} = V_{C2} \end{cases} \tag{26}$$

Besides, the circuit expression of Mode 2 is:

$$\begin{cases} (L + M_1)\left(\frac{di_{L_1}}{dt} + \frac{di_{L_2}}{dt}\right) + 2M_2\frac{di_{L_3}}{dt} + 2M_2\frac{di_{L_4}}{dt} = V_{C1} - V_{in} \\ (L + M_1)\left(\frac{di_{L_3}}{dt} + \frac{di_{L_4}}{dt}\right) + 2M_2\frac{di_{L_1}}{dt} + 2M_2\frac{di_{L_2}}{dt} = V_o - V_{C1} \end{cases} \tag{27}$$

Table 7. The working state of field effect transistor with double switch inductance cascade connection mode.

operating mode	S_1
Mode 1	On
Mode 2	Off

Table 8. The working state of diode in double switch inductance cascade connection mode.

operating mode	D_1	D_2	D_3	D_4	D_5	D_6	D_7
Mode 1	√	×	√	×	√	×	√
Mode 2	×	√	×	√	×	√	×

√：on ×：off

Table 9. The change of inductance current in double switch inductance cascade connection mode.

operating mode	i_{L_1}	i_{L_2}	i_{L_3}	i_{L_4}
Mode 1	+	+	+	+
Mode 2/4	-	-	-	-

+: increase -: decrease

The Analysis of Voltage Gain. According to the circuit expression of Mode 1, the current variations of a and b under Mode 1 can be obtained as Δi_L^+ and Δi_L^-.

$$\begin{cases} \Delta i_L^+ = \frac{V_{in}DT}{(L+M_1+2M_2)} \\ \Delta i_L^- = \frac{(V_{C1}-V_{in})(1-D)T}{2(L+M_1+2M_2)} \end{cases} \tag{28}$$

Similarly, the current changes of c and d are:

$$\begin{cases} \Delta i_L^+ = \frac{V_{C1}DT}{(L+M_1+2M_2)} \\ \Delta i_L^- = \frac{(V_o-V_{C1})(1-D)T}{2(L+M_1+2M_2)} \end{cases} \tag{29}$$

The voltage gain of the converter is:

$$\frac{V_o}{V_{in}} = \frac{(1+\mathrm{D})^2}{(1-\mathrm{D})^2} \tag{30}$$

From the above formula, it can be concluded that compared with the traditional cascaded Boost converter, the converter designed in this paper has a $(1+\mathrm{D})^2$-fold voltage gain increase.

The Analysis of Inductive Current Ripple. Under the premise of uncoupled independent inductance, the steady-state current ripple formula of the converter is as follows:

$$\Delta i_L = \frac{V_{in}DT}{L} \tag{31}$$

In order to reduce the influence of ripple and reduce the volume of magnetic parts, this paper proposes coupling integration of inductors. The mutual inductances of forward coupling are M_1 and M_2, respectively. If the forward coupling coefficients of inductances are k_1 and k_2, respectively, then $k_1 = \frac{M_1}{L}$, $k_2 = \frac{M_2}{L}$.

The current ripple of the coupled inductor is as follows:

$$\Delta i_L = \frac{V_{in}DT}{Lss} \tag{32}$$

Where L_{ss} is the equivalent steady-state inductance.

$$L_{ss}= L\frac{(1+L_1)^2-4k_2^2}{1+k_1-2\frac{1+D}{1-D}k_2} \tag{33}$$

Set a=1/L_{ss}, let the duty cycle $D = 0.6$, when the value of k_2 is between 0.1 and 0.2, the smaller the k_1 is, the smaller the a is ; at the same time, the inductor current ripple is also reduced ; when $k_2 > 0.2$, $a < 0$, meaningless ; it can be seen that when the value range of m is between 0 and 0.2, the smaller the value of k_2 is, the smaller the value of a is. The inductor current ripple is also reduced.

2.4 Summary

The voltage gains from the above analysis are summarized in Table 10.

Table 10. Voltage gain comparison of various connection modes of magnetic integrated switched inductor Boost converter

Coupling means	Voltage gain
Traditional boost converter	$\frac{1}{1-D}$
Interleaved parallel connection mode	$\frac{2}{1-D}$
Single tube cascade connection mode	$\frac{1+D}{(1-D)^2}$
Double tube cascade connection mode	$\frac{(1+\mathrm{D})^2}{(1-\mathrm{D})^2}$

3 Conclusion

In this paper, a high gain Boost converter with switched inductors is introduced. DC boost converter based on switched inductor has the advantage of higher voltage gain and smaller inductor current value. In this paper, the topology and working modes of the three different connection modes are analyzed, and the voltage gain and inductance current ripple of the three different connection modes are obtained. Compared with the traditional Boost converter, the proposed converter has the following advantages:

The voltage gain of the improved converter can be increased obviously in different connection modes, and the maximum can be reached $\frac{(1+\mathrm{D})^2}{(1-\mathrm{D})^2}$.

By using magnetic integration technology, the inductor current ripple can be reduced and the response speed of the converter can be increased by tightly coupling the discrete inductors.

To sum up, the proposed converter has good electrical performance, suitable for fuel cell, photovoltaic power generation and other needs of high-gain DC-DC converter of new energy systems industry.

Authors Contribution

All the authors contributed equally and their names were listed in alphabetical order.

References

1. S.F.Liu, J.Long, T.Fang: Wind and solar complementary new energy has become a new trend. Electrical Engineering, no. 12, pp. 69-71(2008).
2. H.X.Yao, H.Hai, Y.Gao, et al: Novel cascade magnetically integrated switched inductance high gain Boost converter. Journal of Power Supply, vol. 19, no. 06, pp. 111-120(2021).
3. Q.H.Kang: Study on high gain Boost converter with interleaved parallel magnetic integrated switched inductance. Liaoning Technical University(2017).
4. W. Li and X. He: Review of Nonisolated High-Step-Up DC/DC Converters in Photovoltaic Grid-Connected Applications. Ieee Transactions on Industrial Electronics, Article vol. 58, no. 4, pp. 1239-1250(2011).
5. Q.M.Luo, W.Gao, X.Y.Lv, et al: Topology analysis of coupled inductance high gain Boost converter. Proceedings of the CSEE, vol. 37, no. 24, pp. 7266-7275+7441 (2017).
6. Q.M.Luo, B.X.Zhu, L.W.Zhou,Y.Wang: A multi-input high-boost Boost converter. Proceedings of the CSEE, vol. 32, no. 03, pp. 9-14+22(2012).
7. D.C.Du, L.Tian, M.M.Zhao, W.Bao, Y.Chen: Design of novel high-gain Boost converter. Journal of Shaanxi University of Technology(Natural Science Edition, vol. 31, no. 01, pp. 22-25(2015)
8. T.Wang, Y.Tang, Y.H.He, D.J.Fu: Multiunit switched inductor/switched capacitor active network converter. Proceedings of the CSEE, vol. 34, no. 06, pp. 832-838(2014)
9. Q. Zhao, F. C. Lee: High-efficiency, high step-up DC-DC converters. Ieee Transactions on Power Electronics, Article vol. 18,
10. S. M. Dwari, L. Parsa, Ieee: A novel high efficiency high power interleaved coupled-inductor boost DC-DC converter for hybrid and fuel cell electric vehicle. IEEE Vehicle Power and Propulsion Conference (VPPC), Arlington, TX, 2007, pp. 399-404(2007)
11. S.W.Gao, B.Wang, X.T.Sun: A novel magnetic integration technique for interleaved parallel bidirectional DC-DC converter. Proceedings of the CSEE, vol. 43, no. 09, pp. 3538-3550(2023)
12. K. A. Singh, A. Prajapati, K. Chaudhary:High-Gain Compact Interleaved Boost Converter With Reduced Voltage Stress for PV Application. Ieee Journal of Emerging and Selected Topics in Power Electronics, Article vol. 10, no. 4, pp. 4763-4770(2022)
13. H.Z.Li, X.L.Zhu, Q.H.Kang: Study on high gain Boost converter with interleaved parallel magnetic integrated switched inductance. Journal of Power Supply, vol. 19, no. 03, pp. 8-16(2021).
14. J.Ren: Research on magnetic integrated high-gain single-tube cascade Boost converter. Liaoning Technical University(2019)
15. D.S.Rong, J.Ren, B.Ning, et al: Magnetically integrated switched inductance high gain cascade Boost converter. Journal of Power Supply, vol. 19, no. 03, pp. 1-7(2021).